Eur. Phys. J. B **44**, 93–100 (2005)
DOI: 10.1140/epjb/e2005-00103-x

THE EUROPEAN PHYSICAL JOURNAL B

Mesoscopic spin-flip transport through a quantum dot system responded by ac magnetic fields

Hong-Kang Zhao[1,2,a] and Jian Wang[1]

[1] Department of Physics, The University of Hong Kong, Pokfulam Road, Hong Kong, China
[2] Department of Physics, Beijing Institute of Technology, Beijing 100081, China

Received 23 November 2004 / Received in final form 21 December 2004
Published online 16 April 2005 –

Abstract. We investigate mesoscopic spin transport through a quantum dot (QD) responded by a rotating and an oscillating magnetic fields. The rotating magnetic field rotates with the angular frequency ω_0 around the z-axis with the tilt angle θ, while the time-oscillating magnetic field is located in the z-axis with the angular frequency ω. The spin flip is caused by the rotating magnetic field, and it is the major source of spin current. The Zeeman effect is contributed by the two field components, and it is important as the magnetic fields are strong. The oscillating magnetic field takes significant role due to the spin-photon pumping effect, and the spin current can be generated by it even as $\omega_0 \to 0$ for the tilt angle $\theta \neq 0$. The peak and valley structure appears with respect to the frequency ω of oscillating field. The generation of spin current is companying with charge current. Spin current displays quite different appearance between the cases in the absence of source-drain bias ($eV = 0$) and in the presence of source-drain bias ($eV \neq 0$). The symmetric spin current disappears to form asymmetric spin current with a negative valley and a positive plateau. The charge current is mainly determined by the source-drain bias, photon absorption, and spin-flip effect. This system can be employed as an ac charge-spin current generator, or ac charge-spin field effect transistor.

PACS. 85.35.-p Nanoelectronic devices – 73.23.-b Electronic transport in mesoscopic systems – 72.25.Mk Spin transport through interfaces – 73.21.La Quantum dots

1 Introduction

Spintronics is one of the most attractive investigation frontier both for the theoretical and experimental aspects due to the potential application of nano-devices. The spin polarized resonant transport through a ferromagnetic film enhances the nonequilibrium spin population due to the spin accumulation [1,2]. The concept of spin coherent field effect transistor was proposed associated with the spin precession due to the spin-orbit coupling in narrow-gap semiconductors [3]. These could make us to consider the application of spin degree of freedom analog to the charge transport. Recent experiments on the control and manipulation of spin made it possible for the application of spintronic nano-devices [4,5]. The time-resolved optical Faraday rotation measurements demonstrated the coherent spontaneous electron spin and large nuclear magnetic fields in the ferromagnet-semiconductor system [6]. A theory of generation of the electron spin coherence and population in an n-doped ferromagnet-semiconductor system has been presented [7]. The spin-current circuit and generator phenomena are also proposed to develop the spintronics, such as the spin-battery proposals [8–10]. The conductance through a local nuclear spin precessing in a magnetic field has been studied, and the conductance oscillation is found due to the spin-flip coupling between the electrons on the spin site and the leads. The conductance oscillation is composed of ω_L and $2\omega_L$ components of oscillations, where ω_L is the Larmor frequency [11]. In reference [12], the spin field effect transistor (SFET) is presented to be induced by a rotating external magnetic field without involving magnetic materials. The generated spin current is tunable by the gate voltage. As the source-drain bias is removed, the charge current is zero, but the spin current is nonzero. This can make us to operate the spin current purely. The mechanism of the spin current generation is the spin-flip effect of the local electron in the quantum dot (QD).

In this paper, we deal with the spin and charge transports through a quantum dot applied with a rotating magnetic field $\mathbf{B}_0$ and an oscillating magnetic field $\mathbf{B}_1$. The spin-flip is induced by the applied tilting magnetic field which is also rotating around the z-axis. The Zeeman split provides novel channels for electron to tunnel in addition to the original channels of QD. The coupling of spin-up and spin-down components causes novel transport in the

[a] e-mail: zhaohonk@yahoo.com

nonmagnetic material system. The off-diagonal elements of Green's function in spin space are resulted from spin-flip effect, which induces the spin current in the presence of rotating magnetic field. The oscillating magnetic field is a non-collinear magnetic field with the rotating magnetic field, and it is physically interesting to see the compound effects caused by these magnetic fields. The spin-flip effect may cause asymmetric effect, and the oscillating magnetic field induces novel side-bands. The pumped electrons form photon-assisted spin and charge currents. The mesoscopic tunnelling is therefore controlled by the external rotating and oscillating magnetic fields, which can make us to consider oscillating field effect spin-charge devices. Section 2 presents the system formalism and formula derivation. The Landauer-Büttiker-like formula is given there. Numerical calculations are performed in Section 3. Charge and spin currents are displayed as the source-drain bias is zero and nonzero. Brief discussion and concluding remarks are arranged in the final section.

2 Hamiltonian and formalism

The rotating magnetic field rotates with the angular frequency ω_0 around the z-axis with the tilt angle θ, and the azimuthal angle $\varphi(t) = \omega_0 t$, i.e., $\mathbf{B}_0 = \mathrm{B}_0(\sin\theta\cos\varphi(\mathrm{t})\mathbf{e}_\mathrm{x} + \sin\theta\sin\varphi(\mathrm{t})\mathbf{e}_\mathrm{y} + \cos\theta\mathbf{e}_\mathrm{z})$. The time-oscillating magnetic field $\mathbf{B}_1$ located in the z-axis is defined as $\mathbf{B}_1(\mathrm{t}) = \mathrm{B}_1\cos(\omega\mathrm{t})\mathbf{e}_\mathrm{z}$, where ω is the angular frequency of the oscillating magnetic field. The total magnetic field applied to the QD is $\mathbf{B} = \mathbf{B}_0 + \mathbf{B}_1$. We consider the single level QD system, and neglect the intra-dot electron interaction. The Hamiltonian of our system is given as

$$H = \sum_{\gamma k\sigma} \epsilon_{\gamma,k\sigma} c^\dagger_{\gamma,k\sigma} c_{\gamma,k\sigma} + \sum_{\sigma\sigma'} d^\dagger_\sigma \Omega_{\sigma\sigma'}(t) d_{\sigma'} + \sum_\sigma \tilde{E}_\sigma(t) d^\dagger_\sigma d_\sigma + \sum_{\gamma k\sigma} (V_{\gamma k} c^\dagger_{\gamma,k\sigma} d_\sigma + \mathrm{H.c.}), \quad (1)$$

where

$$\mathbf{\Omega}(\mathrm{t}) = \gamma_0 \begin{pmatrix} \cos\theta, & \sin\theta e^{-i\varphi(t)} \\ \sin\theta e^{i\varphi(t)}, & -\cos\theta \end{pmatrix}, \quad (2)$$

and $\tilde{E}_\sigma(t) = E_\sigma + \boldsymbol{\mu}\cdot\mathbf{B}_1(\mathrm{t})$, $E_\sigma = E^{(0)}_\sigma + eV_g, \gamma_0 = \mu_0 B_0$. The operators $c^\dagger_{\gamma,k\sigma}$ ($c_{\gamma,k\sigma}$), and $d^\dagger_\sigma$ (d_σ) are the creation (annihilation) operators of electron in the two leads and the central QD, respectively. In the Hamiltonian, $E^{(0)}_\sigma$ is the energy level of QD in the absence of magnetic field, V_g is the gate voltage, and $\boldsymbol{\mu}\cdot\mathbf{B}_1(\mathrm{t})$ is the Zeeman energy. $\epsilon_{\gamma,k\sigma}$ is the energy of electron in the γth lead, and it is spin degenerate. The magnetic moment of the $\hbar/2$ particle is $\boldsymbol{\mu} = \mu_0\boldsymbol{\sigma}$, $\mu_0 = g\mu_B/2$, where g is the gyromagnetic ratio, μ_B is the Bohr magneton, and $\boldsymbol{\sigma}$ is the Pauli operator. Therefore, $\tilde{E}_\sigma(t) = E_\sigma + \lambda_\sigma\mu_0 B_1\cos(\omega t)$, where λ_σ is eigenvalue of the Pauli operator σ_Z , and it takes the values ±1 for spin-up and spin-down situations. The magnetic field $\mathbf{B}(\mathrm{t})$ induces three effects: the spin-flip; the oscillation of phase factor; the Zeeman splitting of energy levels. This system corresponds to the one that the QD is connected to two electrodes, and the spin-flip effect takes place due the magnetic field $\mathbf{B}_0$.

In order to handle the problem conveniently, we make the gauge transformation for the wave function $\Psi(t) = \hat{U}(t)\tilde{\Psi}(t)$, and Hamiltonian $\tilde{H} = \hat{U}(t)^{-1}H\hat{U}(t)$ in the Schrödinger equation. The unitary operator is defined by $\hat{U}(t) = \exp[-i\Lambda\sum_\sigma \lambda_\sigma \sin(\omega t) d^\dagger_\sigma d_\sigma]$, where $\Lambda = \mu_0 B_1/\hbar\omega$. From the unitary transformation, we can remove the time-oscillating Zeeman energy into the interaction terms, and get the transformed Hamiltonian

$$\tilde{H} = \sum_{\gamma k\sigma} \epsilon_{\gamma,k\sigma} c^\dagger_{\gamma,k\sigma} c_{\gamma,k\sigma} + \sum_{\sigma\sigma'} d^\dagger_\sigma \tilde{\Omega}_{\sigma\sigma'}(t) d_{\sigma'} + \sum_\sigma E_\sigma d^\dagger_\sigma d_\sigma + \sum_{\gamma k\sigma} [\tilde{V}_{\gamma k,\sigma}(t) c^\dagger_{\gamma,k\sigma} d_\sigma + \mathrm{H.c.}]. \quad (3)$$

In the Hamiltonian (3), the interaction strengths are changed to the time-dependent ones as $\tilde{V}_{\gamma k,\sigma}(t) = V_{\gamma k}\exp[-i\lambda_\sigma\Lambda\sin(\omega t)]$. The matrix $\tilde{\mathbf{\Omega}}(t)$ takes the form as in equation (2), but with the transformation as $\varphi(t) \to \tilde{\varphi}(t) = \omega_0 t + \alpha_1\sin(\omega t)$, where $\alpha_1 = 2\Lambda$.

The spin current can be derived from the motion of spin operator of lead in the second quantization picture for our system. We define the spin operator of the αth lead as $\hat{S}_{\alpha,\mu\nu} = \frac{\hbar}{2}\sum_k c^\dagger_{\alpha,k\mu} c_{\alpha,k\nu}\sigma_{\mu\nu}$, and the spin operator of the central QD as $\hat{S}_{\mu\nu} = \frac{\hbar}{2} d^\dagger_\mu d_\nu \sigma_{\mu\nu}$, where $\sigma_{\mu\nu}$ is the Pauli operator matrix, and μ, ν are the spin indices. In the presence of spin-flip effect, the spin current is not conserved, and the usual derivation from Heisenberg equation results in additional term. Detailed discussions are given in the papers where the Rashba spin-orbit interaction effects are analyzed [13,14]. Experimentally, the spin current is measured in the leads by injecting spin-up and spin-down electrons. In our system, the spin current in a lead can be derived through equation of motion of spin operator in the lead $\hat{S}_{\gamma,\mu\nu}$, since there is no spin-flip, or spin-orbit interaction in the leads. This means that there is no spin generation in the leads, and the continuity equation gives $\partial\hat{S}_{\gamma,\mu\nu}/\partial t + \hat{I}_{\gamma,\mu\nu}(t)\mathbf{s}_{\mu\nu} = 0$, where $\mathbf{s} = \hbar\boldsymbol{\sigma}/2$, and $\hat{I}_{\gamma,\mu\nu}(t)$ is the current operator in the γth lead associated with spin indices μ, ν defined by

$$\hat{I}_{\gamma,\mu\nu}(t) = \frac{i}{\hbar}\sum_k \left[\tilde{V}_{\gamma k,\nu} c^\dagger_{\gamma,k\mu}(t) d_\nu(t) - \tilde{V}^*_{\gamma k,\mu} d^\dagger_\mu(t) c_{\gamma,k\nu}(t)\right]. \quad (4)$$

The current is determined by taken the expectation value over quantum state and grand canonical ensemble expectation, i.e., $I_{\gamma,\mu\nu}(t) = \langle\hat{I}_{\gamma,\mu\nu}(t)\rangle$. The electric current operator is defined by $\hat{I}_{\alpha,e} = e\sum_\sigma \hat{I}_{\alpha,\mu\mu}$, and the spin current operator is $\hat{I}_{\alpha,s} = \sum_{\mu\nu}\hat{I}_{\alpha,\mu\nu}\mathbf{s}_{\mu\nu}$. We are interested in the spin current of the $\mathbf{s}^\mathrm{z}$ components tunnelling from the leads to QD, which is associated with the injection of currents $I_{\alpha,\downarrow\downarrow}$ and $I_{\alpha,\uparrow\uparrow}$ from opposite directions, and the spin current is given by $I^z_{\alpha,s} = \sum_\mu I_{\alpha,\mu\mu}\mathbf{s}^\mathrm{z}_{\mu\mu}$. In the central

QD, spin flip takes place, and the spin generation causes additional terms in the continuity equation

$$\frac{\partial \hat{S}^z_{\sigma\sigma}}{\partial t} = \left\{ \frac{i}{\hbar}\left[\tilde{\Omega}_{\bar{\sigma}\sigma} d^\dagger_{\bar{\sigma}} d_\sigma - \tilde{\Omega}_{\sigma\bar{\sigma}} d^\dagger_\sigma d_{\bar{\sigma}}\right] + \sum_\gamma \hat{I}_{\gamma,\sigma\sigma}(t) \right\} \mathbf{s}^z_{\sigma\sigma}. \tag{5}$$

The notation $\bar{\sigma}$ denotes the spin variable by making spin flipping versus σ, i.e., if d_σ represents spin-up electron, the notation $d_{\bar{\sigma}}$ represents spin-down electron. The source terms can not be cancelled by summing up the spin variable σ in the above equation, and thus the spin current is non-conservative in our system. Nevertheless, the charge current is conserved to satisfy the continuity equation $\partial\hat{Q}/\partial t = e\sum_{\gamma\sigma}\hat{I}_{\gamma,\sigma\sigma}(t)$, where $\hat{Q} = e\sum_\sigma d^\dagger_\sigma d_\sigma$ is the charge operator of QD. The detailed spin current is strongly dependent on the structure of concrete system. We define the Green's function $G^X_{\sigma\sigma'}(t,t')$ $(X \in \{r,a,<\})$ of the coupled QD corresponding to the retarded, advanced and Keldysh Green's functions [15–17]. The retarded (advanced) Green's function is defined by

$$G^{r(a)}_{\sigma\sigma'}(t,t') = \mp\frac{i}{\hbar}\theta(\pm t \mp t')\left\langle [d_\sigma(t), d^\dagger_{\sigma'}(t')]_+ \right\rangle.$$

The Keldysh Green's function is defined by

$$G^<_{\sigma\sigma'}(t,t') = \frac{i}{\hbar}\left\langle d^\dagger_{\sigma'}(t') d_\sigma(t)\right\rangle.$$

The notation $\langle ... \rangle$ represents quantum expectation value and ensemble average. The spin and charge current components in the γth lead can be expressed by the Green's functions $G^X_{\sigma\sigma'}(t,t')$ and the self-energy matrices $\Sigma^X_{\gamma\sigma\sigma'}(t,t')$ as

$$\begin{aligned} I_{\gamma,\mu\nu}(t) = \int dt_1 [& G^r_{\nu\mu}(t,t_1)\Sigma^<_{\gamma,\mu\nu}(t_1,t) \\ & + G^<_{\nu\mu}(t,t_1)\Sigma^a_{\gamma,\mu\nu}(t_1,t) + [G^<_{\mu\nu}(t,t_1)\Sigma^a_{\gamma,\nu\mu}(t_1,t) \\ & + G^r_{\mu\nu}(t,t_1)\Sigma^<_{\gamma,\nu\mu}(t_1,t)]^*. \end{aligned} \tag{6}$$

The self-energy of the γth lead is defined by $\Sigma^X_{\gamma,\mu\nu}(t_1,t) = \sum_k \tilde{V}^*_{\gamma k,\mu}(t_1)\tilde{V}_{\gamma k,\nu}(t) g^X_{\gamma,k\mu}(t_1,t)$, where $g^X_{\gamma k,\sigma}(t_1,t)$, $(X \in \{r,a,<\})$, is the Green's function of the γth lead.

In the absence of alternating magnetic field component as $\mathbf{B}_1 = 0$, and without the spin-flip effect, the Green's function of the isolated QD in the applied static magnetic field component $\mathbf{B}_0$ is expressed as $g^r_{\sigma\sigma'}(t,t') = -\frac{i}{\hbar}\Theta(t-t')\exp[-\frac{i}{\hbar}\varepsilon_\sigma(\theta)(t-t')]\delta_{\sigma\sigma'}$, where $\varepsilon_\sigma(\theta) = E_\sigma + \lambda_\sigma\gamma_0\cos\theta$. The energy level of QD is split due to the applied static Zeeman magnetic field, which is dependent on the tilt angle θ. From the equation of motion, the retarded Green's function of electron in QD can be derived to satisfy the Dyson-like equation

$$\begin{aligned} G^r_{\sigma\sigma'}(t,t') = g^r_{\sigma\sigma'}(t,t') + & \int dt_1 g^r_{\sigma\sigma}(t,t_1)\tilde{\Omega}_{\sigma\bar{\sigma}}(t_1) G^r_{\bar{\sigma}\sigma'}(t_1,t') \\ & + \int\int dt_1 dt_2 g^r_{\sigma\sigma}(t,t_1)\Sigma^r_{\sigma\sigma}(t_1,t_2) G^r_{\sigma\sigma'}(t_2,t'). \end{aligned} \tag{7}$$

The spin-flip effect is contained in the second term of equation (7) through the interaction strength $\tilde{\Omega}_{\sigma\bar{\sigma}}(t_1)$, which does not disappear even if $\omega_0 \to 0$. Similarly, one can obtain the Dyson-like equation for the Keldysh Green's function. From the equation of motion, and by using the formulas of Jauho et al. in reference [15], we have the integral equation

$$\begin{aligned} G^<_{\sigma\sigma'}(t,t') = & \int dt_1 g^r_{\sigma\sigma}(t,t_1)\tilde{\Omega}_{\sigma\bar{\sigma}}(t_1) G^<_{\bar{\sigma}\sigma'}(t_1,t') \\ & + \int\int dt_1 dt_2 g^r_{\sigma\sigma}(t,t_1)[\Sigma^r_{\sigma\sigma}(t_1,t_2) G^<_{\sigma\sigma'}(t_2,t') \\ & + \Sigma^<_{\sigma\sigma}(t_1,t_2) G^a_{\sigma\sigma'}(t_2,t')]. \end{aligned} \tag{8}$$

The information of spin-flip effect is contained in the first term of equation (8) due to the coupling $\tilde{\Omega}_{\sigma\bar{\sigma}}(t_1)$ stated in equation (3), which is determined by the nonzero off-diagonal Green's functions $G^X_{\bar{\sigma}\sigma}$ in spin space. $\Sigma^X_{\sigma\sigma'}(t_1,t_2)$ is the total self-energy of leads defined by the summation of self-energies of leads as $\Sigma^X_{\sigma\sigma'}(t_1,t_2) = \sum_\gamma \Sigma^X_{\gamma,\sigma\sigma'}(t_1,t_2)$. We make Fourier transformation over the two times t, t', and solve the time-averaged spin and charge currents. From equation (7), we obtain the quasi-equilibrium retarded Green's function of QD

$$\begin{aligned} G^r_{\sigma\sigma'}(\epsilon,\epsilon') = & G^r_{\sigma\sigma}(\epsilon)[\delta_{\sigma\sigma'}\delta(\epsilon-\epsilon') + \gamma(\theta) \\ & \times \sum_n J_n(\alpha_1)\tilde{g}^r_{\bar{\sigma}\bar{\sigma}}(\tilde{\epsilon}_{n\sigma})\delta(\tilde{\epsilon}_{n\sigma}-\epsilon')\delta_{\bar{\sigma}\sigma'}], \end{aligned} \tag{9}$$

where $\gamma(\theta) = \gamma_0\sin\theta$, $\tilde{\epsilon}_{n\sigma} = \epsilon - \lambda_\sigma(\omega_0 + n\omega)\hbar$, $(n = 0, \pm1, \pm2, ...)$. The diagonal retarded Green's function is related to

$$G^r_{\sigma\sigma}(\epsilon) = \frac{1}{\epsilon - \varepsilon_\sigma(\theta) - \Pi^r_\sigma(\epsilon)}, \tag{10}$$

where $\Pi^r_\sigma(\epsilon) = \Sigma^r_{\sigma\sigma}(\epsilon) + \gamma(\theta)^2\sum_n J^2_n(\alpha_1)\tilde{g}^r_{\bar{\sigma}\bar{\sigma}}(\tilde{\epsilon}_{n\sigma})$, and $\alpha_1 = 2\mu_0 B_1/\hbar\omega$. The Bessel function of the first kind $J_n(x)$ is involved in the Green's functions. We have defined the Green's function $\tilde{g}^r_{\sigma\sigma}(\epsilon) = 1/[\epsilon - \varepsilon_\sigma(\theta) - \Sigma^r_{\sigma\sigma}(\epsilon)]$. The first term in equation (9) gives the diagonal elements of retarded Green's function, while the second term gives the off-diagonal elements of retarded Green's function in spin space. Note that the diagonal elements of the retarded Green's function contain the spin-flip effect included in $\Pi^r_\sigma(\epsilon)$ through the term possessing $\tilde{g}^r_{\bar{\sigma}\bar{\sigma}}(\epsilon)$. This spin-flip term disappears as $\theta = n\pi$, $(n = 0, \pm1, \pm2, ...)$. The Zeeman energy induced by the tilted magnetic field $\mathbf{B}_0$ is $\lambda_\sigma\gamma_0\cos\theta$, while the spin flip causes different kind of energy splitting as $\lambda_\sigma(\omega_0 + n\omega)\hbar$ associated with the frequencies of the two fields ω_0, and ω. The local electrons in the QD absorb photons of the rotating and oscillating magnetic fields. For the rotating field, only single photon absorption procedure takes place, while for the oscillating magnetic field, multi-photon absorption procedure can occur. This also indicates that the rotating field and the oscillating field contain different characteristics, and they can not be simply cancelled from each other. Similarly, the quasi-equilibrium Keldysh Green's function

of QD can be derived from equation (8) as

$$G^{<}_{\sigma\sigma'}(\epsilon,\epsilon') = G^{r}_{\sigma\sigma}(\epsilon)[\Sigma^{<}_{\sigma\sigma}(\epsilon)G^{a}_{\sigma\sigma'}(\epsilon,\epsilon') + \gamma(\theta) \times \sum_{n} J_n(\alpha_1)\Sigma^{<}_{\bar{\sigma}\bar{\sigma}}(\tilde{\epsilon}_{n\sigma})\tilde{g}^{r}_{\bar{\sigma}\bar{\sigma}}(\tilde{\epsilon}_{n\sigma})G^{a}_{\bar{\sigma}\sigma'}(\tilde{\epsilon}_{n\sigma},\epsilon')]. \quad (11)$$

The self-energy $\Sigma^{X}_{\sigma\sigma}(\epsilon)$ in above formulas is defined as $\Sigma^{X}_{\sigma\sigma}(\epsilon) = \sum_{\gamma kn} \mid V_{\gamma k} \mid^2 J^2_n(\Lambda) g^{X}_{\gamma,k\sigma}(\epsilon - n\hbar\omega)$. In the self-energies of leads, we have defined the Fourier transformed Green's functions of leads as $g^{r(a)}_{\gamma,k\sigma}(\epsilon) = 1/[\epsilon - \epsilon_{\gamma,k\sigma} \pm i\eta]$, $(\eta \to 0)$, and $g^{<}_{\gamma,k\sigma}(\epsilon) = 2\pi i f_\gamma(\epsilon)\delta(\epsilon - \epsilon_{\gamma,k\sigma})$. The Fermi distribution function of the γth lead is $f_\gamma(\epsilon) = 1/\{\exp[(\epsilon - \mu_\gamma)/K_BT] + 1\}$, where μ_γ is the chemical potential of the γth lead, and K_B is the Boltzmman constant. The Keldysh self-energy is given by $\Sigma^{<}_{\sigma\sigma}(\epsilon) = i\sum_{\gamma n} \Gamma_\gamma(\epsilon - n\hbar\omega)J^2_n(\Lambda)f_\gamma(\epsilon - n\hbar\omega)$, where $\Gamma_\gamma(\epsilon) = 2\pi\sum_k \mid V_{\gamma k} \mid^2 \delta(\epsilon - \epsilon_{\gamma,k\sigma})$ is the line-width of the γth lead. The first term of Keldysh Green's function in equation (11) takes the form of $G^{<} = G^r\Sigma^{<}G^a$ given by Jauho et al. in reference [15]. However, the second term in equation (11) also contributes to the diagonal elements of the Keldysh Green's function through the off-diagonal elements of Green's function $G^{a}_{\bar{\sigma},\sigma}$. The diagonal elements of Keldysh Green's function are therefore determined by

$$G^{<}_{\sigma\sigma}(\epsilon) = \mid G^{r}_{\sigma\sigma}(\epsilon) \mid^2 \left[\Sigma^{<}_{\sigma\sigma}(\epsilon) + \gamma^2(\theta) \times \sum_{n} J^2_n(\alpha_1)\Sigma^{<}_{\bar{\sigma}\bar{\sigma}}(\tilde{\epsilon}_{n\sigma}) \mid g^{r}_{\bar{\sigma}\bar{\sigma}}(\tilde{\epsilon}_{n\sigma}) \mid^2 \right]. \quad (12)$$

The Zeeman splitting, photon absorption, and spin-flip effect contain in the Green's functions above.

Making Fourier transformation over the current equation (6), and substituting the Fourier transformed self-energy matrices into it, we can derive the current formula in Fourier space. We are interested in the time-averaged tunnelling current, and only consider the diagonal current $I_{\gamma,\sigma\sigma}$ in spin space, since it is associated with experiments. Thus, we obtain the time-averaged diagonal elements of current formula of the γth lead in spin space

$$I_{\gamma,\sigma\sigma} = -\frac{2}{h}Im\int d\epsilon \sum_{n} J^2_n(\Lambda)\Gamma_\gamma(\epsilon - n\hbar\omega) \times \left[f_\gamma(\epsilon - n\hbar\omega)G^{r}_{\sigma\sigma}(\epsilon) + \frac{1}{2}G^{<}_{\sigma\sigma}(\epsilon)\right], \quad (13)$$

where $G^{r}_{\sigma\sigma}(\epsilon)$, and $G^{<}_{\sigma\sigma}(\epsilon)$ are the diagonal elements of retarded and Keldysh Green's functions given by equations (10) and (12). We have used the notation $G^{X}_{\sigma\sigma}(\epsilon,\epsilon') = G^{X}_{\sigma\sigma}(\epsilon)\delta(\epsilon - \epsilon')$ for the diagonal Green's functions. Since the diagonal elements of the Green's functions are determined by the off-diagonal elements of Green's functions in spin space, this current formula contains the information of spin-flip effect as $\theta \neq n\pi$, $(n = 0, \pm1, \pm2, ...)$. In the wide-band limit, the line-widths of leads are energy-independent Γ_γ. The retarded self-energy is determined by the imaginary part $\Sigma^{r}_{\sigma\sigma}(\epsilon) = -i\Gamma/2$, where $\Gamma = \Gamma_L + \Gamma_R$. The charge current of the γth lead is the summation of spin-up and spin-down current components $I_{\gamma,e} = e(I_{\gamma,\uparrow\uparrow} + I_{\gamma,\downarrow\downarrow})$, and the $\mathbf{s}^z$ spin current is defined by $I_{\gamma,s} = \hbar(I_{\gamma,\downarrow\downarrow} - I_{\gamma,\uparrow\uparrow})/2$ corresponding to the notation of spin-up $\uparrow$ and spin-down $\downarrow$. Substituting the corresponding Green's functions into the current formula (13), we obtain the diagonal elements of current as $I_{\gamma,\sigma\sigma} = I^{(1)}_{\gamma,\sigma\sigma} + I^{(2)}_{\gamma,\sigma\sigma}$. The first part of current is given by the Landauer-Büttiker-like formula [18,19]

$$I^{(1)}_{\gamma,\sigma\sigma} = \frac{1}{h}\sum_{n\ell\beta}\int d\epsilon T_{\gamma\beta\sigma,n\ell}(\epsilon)[f_\gamma(\epsilon - n\hbar\omega) - f_\beta(\epsilon - \ell\hbar\omega)], \quad (14)$$

where $T_{\gamma\beta\sigma,n\ell}(\epsilon) = \Gamma_\gamma\Gamma_\beta J^2_n(\Lambda)J^2_\ell(\Lambda) \mid G^{r}_{\sigma\sigma}(\epsilon) \mid^2$ represents the transmission coefficient of electron with spin σ transporting from γth lead to the βth lead. The scattering-matrix approach on phase-coherent transport through a spin degenerate system was generalized to nonlinear ac transport by Pedersen and Büttiker [20]. They presented a theory of photon-assisted electron transport, in which charge and current conservation are satisfied for all Fourier components of the current. In equation (14), spin-flip effect is contained in tunnelling current components through the Green's function of QD $G^{r}_{\sigma\sigma}(\epsilon)$. The spin-flip effect provides novel channels other than the Zeeman splitting effect. This part of current is conserved as $\sum_{\gamma\sigma} I^{(1)}_{\gamma,\sigma\sigma} = 0$, which can be seen directly by changing the indices n and ℓ, and by employing the symmetry of transmission coefficient $T_{\gamma\beta\sigma,n\ell}(\epsilon) = T_{\beta\gamma\sigma,\ell n}(\epsilon)$. One also observes that this part of current vanishes as $\mu_R = \mu_L$. The second part of tunnelling current $I^{(2)}_{\gamma,\sigma\sigma}$ is determined by

$$I^{(2)}_{\gamma,\sigma\sigma} = \frac{1}{h}\sum_{nm\ell\beta}\int d\epsilon J^2_m(\alpha_1)T_{\gamma\beta\sigma,n\ell}(\epsilon) \mid \tilde{g}^{r}_{\bar{\sigma}\bar{\sigma}}(\tilde{\epsilon}_{m\sigma}) \mid^2 \times \gamma(\theta)^2[f_\gamma(\epsilon - n\hbar\omega) - f_\beta(\tilde{\epsilon}_{m\sigma} - \ell\hbar\omega)]. \quad (15)$$

The spin current is induced by applying the magnetic field $\mathbf{B}$ to form spin flip, and it is intimately associated with the photon absorption procedure. As the oscillating component of magnetic field is zero, the spin current is generated by the rotating field, and this current becomes zero as $\omega_0 \to 0$ [12]. However, one observes that novel pumping spin current appears due to the oscillating magnetic field. The spin current does not disappear even as $\omega_0 \to 0$ for $\theta \neq n\pi$ when $eV = 0$. The mechanism of this situation comes from the spin-flip effect. As the static magnetic field ($\omega_0 = 0$) is applied to the QD, spin-flip effect is induced in the local electrons with the interaction strength $\gamma(\theta)$. The applied oscillating magnetic field then splits the energy level of QD forming side levels for electrons to tunnel. The pumped electrons with different spin variable occupy different channels in the QD, and establish different electron distribution. The asymmetric electron transport through the system forms nonzero net current.

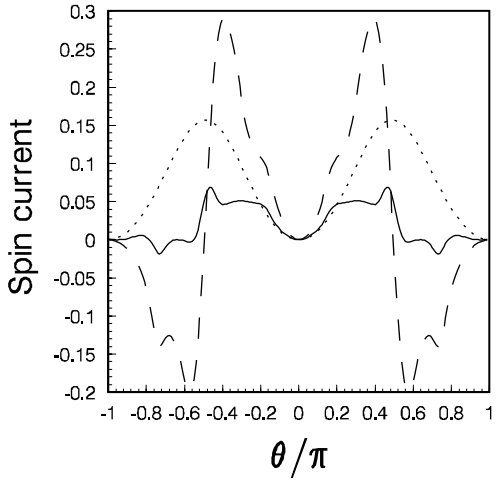

Fig. 1. The spin current in unit I_{s0} versus phase θ as source-drain bias $eV = 0$. The parameters are chosen as $\hbar\omega_0 = 0.1\Delta$, $\gamma_0 = \Delta$ and for the solid curve $\Lambda = 0.6$, $\hbar\omega = 0.6\Delta$, $eV_g = \Delta$; for the dotted curve $eV_g = \Delta, \Lambda = 0$; for the dashed curve $eV_g = 0, \Lambda = 0.6$, $\hbar\omega = 0.6\Delta$.

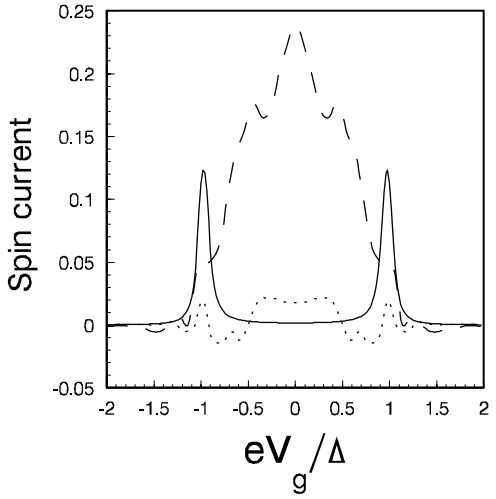

Fig. 2. The spin current in unit I_{s0} versus gate voltage as source-drain bias $eV = 0$. The parameters are chosen as $\hbar\omega_0 = 0.1\Delta$, $\gamma_0 = \Delta$, and $\theta = \pi/3$. The solid curve is related to $\Lambda = 0$; the dotted curve is related to $\Lambda = 0.6, \hbar\omega = 0.3\Delta$; the dashed curve is related to $\Lambda = 0.6, \hbar\omega = 0.6\Delta$.

3 Numerical calculations

We perform the numerical calculation of spin and charge currents at zero temperature for both of the cases as terminal bias $eV = 0$ and $eV \neq 0$. The energy quantity $\Delta = 0.1$ meV is used as the energy scale throughout the calculations. We consider the symmetric system as $\Gamma_L = \Gamma_R = 0.005$ meV, and $E_\sigma^{(0)} = 0$. We define the scaling of spin current as $I_{s0} = \Delta/(4\pi) = 1.59 \times 10^{-2}$ meV, and the scaling of charge current by $I_{c0} = e\Delta/(4h) = 0.96$ nA. The Fermi distribution function becomes the step function at zero temperature as $f_\gamma(\epsilon) = 1 - \Theta(\epsilon - \mu_\gamma)$. We present the charge and spin currents of the left lead by calculating $I_e = e(I_{L,\uparrow\uparrow} + I_{L,\downarrow\downarrow})$, and $I_s = \hbar(I_{L,\downarrow\downarrow} - I_{L,\uparrow\uparrow})/2$.

Figure 1 displays the spin current versus angle θ as $eV = 0$. The spin current varies sensitively with the applied rotating and oscillating magnetic field components. As the oscillating field $\mathbf{B}_1$ is zero, the spin current oscillates periodically with the period π, and the oscillating shape is similar to $\sin^2\theta$. As the oscillating magnetic field is applied, the magnitude and shape of the spin current are affected by the magnitude and frequency ω of the oscillating field, which can be observed from the dashed curve. The spin current is adjusted by the gate voltage V_g obviously. One sees that the completely different oscillation structure appears as the gate bias changes from $eV_g = 0$ to $eV_g = \Delta$.

The spin current resonance versus gate voltage in the absence of source-drain bias is presented in Figure 2 to exhibit the modification of spin current by the oscillating magnetic field component. In the absence of external oscillating field, two resonant peaks are observed to be located at $eV_g = \pm\Delta$, which is already stated in the spin-pumping system [12], and the spin-precessing system [11]. However, as the oscillating field is applied to the system, the resonant structure is modified considerably. The modification of spin current is sensitively associated with the frequency of the applied oscillating field. As the frequency $\omega = 0.6\Delta/\hbar$, a large main resonant peak emerges, and several small side peaks are mounted on the main peak. As $\omega = 0.3\Delta/\hbar$, the spin current is relatively small, and the current structure is quite different compared with the others.

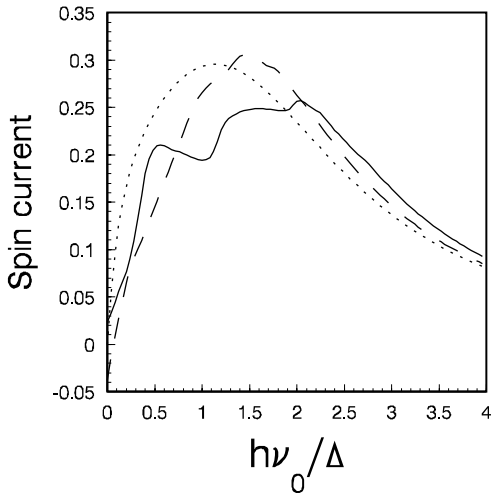

Fig. 3. The spin current in unit I_{s0} versus photon energy $h\nu_0$ of rotating field as source-drain bias $eV = 0$. The parameters are chosen as $eV_g = \Delta$,$\gamma_0 = \Delta$, $\theta = \pi/3$, and for the dotted curve $\Lambda = 0$; for the solid curve $\Lambda = 0.6, \hbar\omega = 0.6\Delta$; for the dashed curve $\Lambda = 0.6, \hbar\omega = 0.3\Delta$.

Figure 3 displays the spin current versus photon energy of the rotating magnetic field $h\nu_0$,($\omega_0 = 2\pi\nu_0$). The photon energy is scaled by Δ. This corresponds to the case that the frequency is scaled by the quantity $\Delta/h = 24.1$ GHz. In the absence of oscillating magnetic

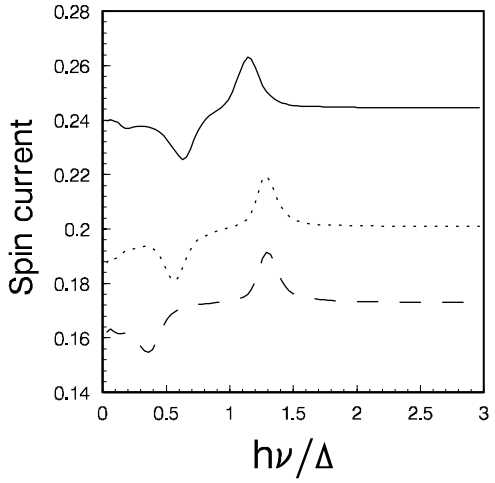

Fig. 4. The spin current in unit I_{s0} versus photon energy $h\nu$ of the oscillating field as $eV_g = \Delta$, $\gamma_0 = \Delta$, and $eV = 0$. The parameters are chosen as $\mu_0 B_1 = 0.36\Delta$, and for the solid curve $\hbar\omega_0 = 0.5\Delta$, $\theta = \pi/3$; for the dashed curve $\hbar\omega_0 = 0.5\Delta$, $\theta = \pi/4$; for the dotted curve $\hbar\omega_0 = 0.3\Delta$, $\theta = \pi/3$.

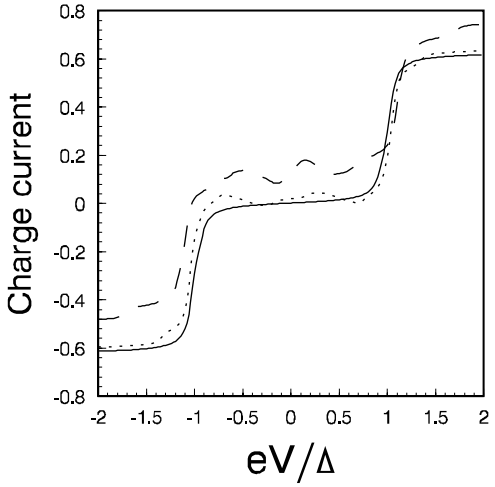

Fig. 5. The charge current-voltage characteristics in unit I_{c0} for the charge current. The parameters are chosen as $\hbar\omega_0 = 0.1\Delta, \theta = \pi/3$, $\gamma_0 = \Delta$, and $eV_g = 0$. The dashed, dotted curves correspond to $\hbar\omega = 0.6\Delta, 0.3\Delta$ as $\Lambda = 0.6$; the solid curve corresponds to $\Lambda = 0$, respectively.

field, one observes that the spin current increases rapidly with the frequency to reach its maximum value at $\nu_0 = \Delta/h$, and then declines monotonically [12]. The nonzero pumped spin current by the oscillating field as $\omega_0 = 0$ is explicitly displayed. The modified and suppressed spin current signifies the spin-photon absorption effect.

The spin current versus the photon energy of the oscillating field $h\nu$ ($\omega = 2\pi\nu$) is depicted in Figure 4. The peak and valley structure appears in the frequency regime as $0 < \nu < 1.5\Delta/h$. As the $\nu \gg 1.5\Delta/h$, the saturate spin current is achieved.This figure shows that the magnitude of spin current is intimately determined by the parameters θ, and ω_0. The peak and valley structure keeps by

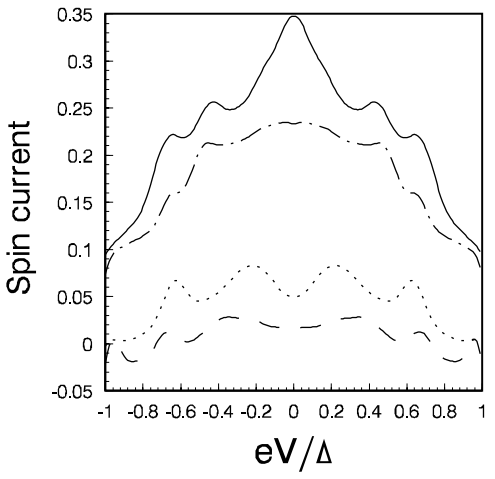

Fig. 6. The spin current in unit $I_{s0}/4$ versus source-drain bias eV. The parameters are chosen as $eV_g = 0, \theta = \pi/3, \hbar\omega_0 = 0.1\Delta, \Lambda = 0.6, \Delta = \gamma_0$, and for the solid curve $\hbar\omega = 0.6\Delta$; for the dashed curve $\hbar\omega = 0.3\Delta$; for the dotted curve $\hbar\omega = 0.4\Delta$; for the dash-dotted curve $\hbar\omega = 0.5\Delta$.

changing the parameters θ, and ω_0, and it comes from the competition of spin-up and spin-down current parts with respect to the frequency ω.

We present the charge current-voltage characteristics in Figure 5 to show the photon-assisted tunnelling and spin-flip effect by changing the source-drain bias eV. The charge current is contributed by the two parts shown in equations (14) and (15). As the magnitude B_1 of oscillating magnetic field approaches zero, two distinct steps appear at $eV = \pm\Delta$. This denotes that the single level of quantum dot is split to form double levels, and the gap between the two levels is $E_g = 2\Delta$, which can be seen from solid curve directly. This situation indicates that the normal metal QD changes to semiconducting QD with energy gap E_g. As the oscillating magnetic field is applied to QD, the charge current is modified due to photon absorption and emission. The spin-flip effect, Zeeman effect, and photon-assisted tunnelling devote together to the charge current. The energy gap E_g disappears due to the electron absorbing photons to form novel channels for electrons to tunnel. This behavior becomes stronger as the frequency of oscillating magnetic field is larger.

The spin current-voltage characteristics are exhibited in Figure 6 to display the influence of the source-drain bias and oscillating magnetic field. As $eV \neq 0$, the spin current is contributed by both of the two parts given in equations (14) and (15). The spin current appears quite differently from the charge current shown in Figure 5. The spin current is symmetric about $eV = 0$, and a resonant peak emerges at $eV = 0$ for the case as $\hbar\omega = 0.6\Delta$. The magnitude of spin current declines with the photon energy, and several hills are mounted on the curves. The shape and magnitude of spin current intimately rely on the photon energy. For example , the spin current exhibits a valley at $eV = 0$ when the photon energy is small (dotted curve), but this valley becomes peak when $\hbar\omega$ is large (solid curve). As $\theta \neq n\pi$, the oscillating magnetic

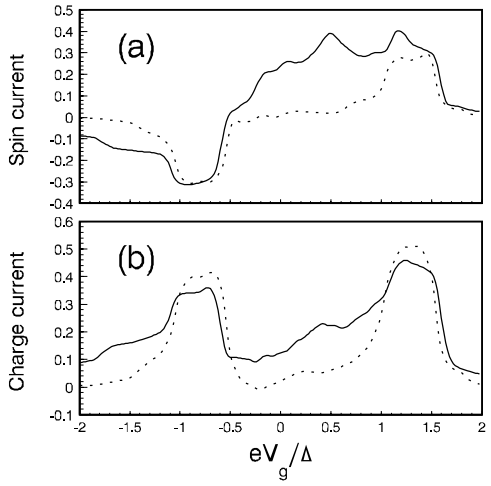

Fig. 7. The spin and charge currents versus gate voltage as $eV = 0.5\Delta$. Diagram (a) is the spin current in unit $I_{s0}/4$, while diagram (b) is the charge current in unit I_{c0}. The parameters are chosen as $\theta = \pi/3, \Lambda = 0.6, \hbar\omega_0 = 0.1\Delta$, and $\Delta = \gamma_0$. The solid and dotted curves are related to $\hbar\omega = 0.6\Delta, 0.3\Delta$, respectively.

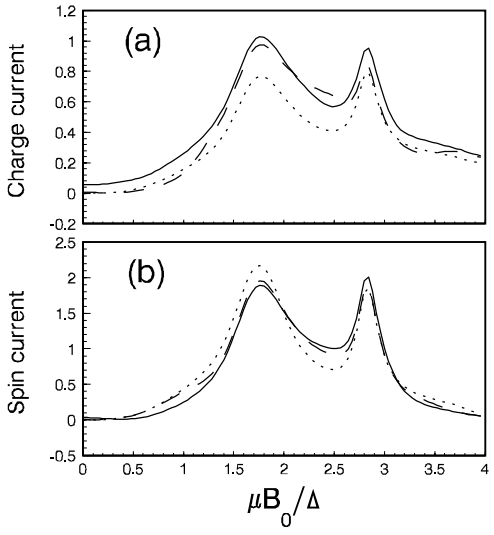

Fig. 8. The spin and charge currents versus Zeeman energy μB_0 at different source-drain biases. Diagram (a) is the charge current in unit I_{c0}, while diagram (b) is the spin current in unit $I_{s0}/4$. The parameters are chosen as $\theta = \pi/3, \Lambda = 0.6, \hbar\omega_0 = 0.1\Delta$, $eV_g = 0$, and $\hbar\omega = \Delta$. The solid, dashed, and dotted curves are related to $eV = 0.5\Delta$, $eV = 0.3\Delta$, and $eV = 0$, respectively.

field acts as a photon-electron pump, and the photon energy induces the additional photon bias to generate spin current. The magnitude of generated spin current is dependent on the photon energy. On the other hand, the photon absorption also induces multi-levels for electron to tunnel through QD, and the positions of photon-induced channels are completely dependent on the photon energy. Therefore, the photon-assisted resonant transport and spin-flip effect determine the mesoscopic spin transport together.

The gate voltage controls charge and spin currents by tuning eV_g, which shows symmetric behavior with respect to the gate voltage at zero source-drain bias (Fig. 2). As comparison, we present the charge and spin currents versus gate voltage in Figure 7 for the case of $eV \neq 0$. One observes that the spin current displays quite different appearance from the case where $eV = 0$. The symmetric spin current disappears to form asymmetric spin current with a negative valley located around $-\Delta$, and a positive plateau emerging at around Δ for the case of photon energy $\hbar\omega = 0.3\Delta$ (dotted curve). When the photon energy becomes larger as $\hbar\omega = 0.6\Delta$, the positive plateau becomes wider, and several small peaks emerge on the plateau. This asymmetric behavior comes from the fact that as $eV \neq 0$, the spin current is contributed by both of the two terms $I^{(1)}_{\gamma,\sigma\sigma}$ and $I^{(2)}_{\gamma,\sigma\sigma}$. The competition of the two terms results in net spin current. The photon-absorption in such system produces asymmetric side-band due to the spin-flip effect, which also induces the asymmetric spin current. We depict the charge current versus gate voltage for $eV \neq 0$ in diagram (b) to see the spin-flip charge transport. We observe that double resonant positive peaks appear around $eV \approx \pm\Delta$ as $\hbar\omega = 0.3\Delta$ (dotted curve). The asymmetric resonant structure is also exhibited in the charge current versus gate voltage. As the photon energy becomes larger, the asymmetric behavior becomes stronger. The reason for the asymmetric behavior of charge current is the same as that of spin current given above.

In Figure 8, we show the spin and charge currents versus the static Zeeman energy μB_0 for different source-drain biases. The photon energy $\hbar\omega = \Delta$ is taken as the energy scale in this figure. Double resonant structure appears in both of the spin and charge currents with the resonant peaks located at $\mu B_0 \approx 1.5\ \Delta$, $2.8\ \Delta$. The resonances of the two currents possess similar structures, but the detailed behaviors are different. Firstly, the spin current is zero as $\mu B_0 = 0$, and then it increases to a resonant peak at $\mu B_0 \approx 1.5\ \Delta$. But for the charge current, it can not be zero as $\mu B_0 = 0$ for $eV \neq 0$. This means that the charge current is mainly determined by the source-drain bias and photon energy in the absence of spin-flip source $\gamma(\theta)$. The charge current for this case is contributed by $I^{(1)}_{\gamma,\sigma\sigma}$ completely, while the spin current is contributed by the term $I^{(2)}_{\gamma,\sigma\sigma}$ completely as $eV = 0$. Secondly, The resonant peaks of charge current are fatter than those of spin current. This indicates that the spin current is affected by Zeeman field B_0 more sensitively than that of the charge current. The resonant values of charge current are larger with respect to larger source-drain bias voltage, while the spin current does not possess this behavior. The peak of zero biased current (dotted curve) can be larger than the source-drain biased ones (solid and dashed curves). This behavior also displays in Figure 6, which shows that the value of spin current decreases with increasing the absolute value of source-drain voltage V.

4 Concluding remarks

The spin flip of QD is the major source of the spin current. The frequencies ω_0, ω are transferred to spin and charge currents. The Zeeman effect is contributed by the rotating and oscillating magnetic fields, and it is important as the magnetic fields are strong. The tilt angle θ of the rotating field governs the appearance of spin current which is zero as $\theta = n\pi$. The oscillating magnetic field takes significant role in the spin and charge currents, and it modifies the spin and charge currents to show quite different behaviors. The spin current can be generated by the oscillating magnetic field as $\omega_0 \to 0$. This system provides a model of device for obtaining spin current by rotating and oscillating magnetic fields. Spin current displays quite different appearance between the cases for $eV = 0$ and $eV \neq 0$. The photon absorption induces multi-levels for electron to tunnel through QD, and the positions of photon-induced channels are completely dependent on the photon energy. The symmetric spin current disappears to form asymmetric spin current with a negative valley and a positive plateau. The charge current is mainly determined by the source-drain bias and photon energy in the absence of spin-flip. In the presence of spin-flip, the charge current is composed of source-drain driven current, the photon-assisted tunnelling, and generated spin-flip electron current. The spin current is affected by Zeeman field B_0 more sensitively than that of the charge current. The resonant values of charge current is larger with respect to larger source-drain bias voltage. Since the system is controlled by the external parameters as gate voltage, source-drain bias, rotating and oscillating magnetic fields, this system can be employed as an ac spin current generator, or an ac charge-spin FET.

This work was supported by a RGC grant from the SAR Government of Hong Kong under Grant No. HKU 7044/04P, by the National Natural Science Foundation of China under the Grant No. 10375007, and by the Fundamental Research Foundation of Beijing Institute of Technology.

References

1. R.H. Silsbee, A. Janossy, P. Monod, Phys. Rev. B **19**, 4382 (1979)
2. M. Johnson, R.H. Silsbee, Phys. Rev. Lett. **55**, 1790 (1985); M. Johnson, Phys. Rev. Lett. **70**, 2142 (1993)
3. S. Datta, B. Das, Appl. Phys. Lett. **56**, 665 (1990)
4. S.A. Wolf et al., Science **294**, 1488 (2001); R. Fiederling et al., Nature (London) **402**, 787 (1999)
5. G.A. Prinz, Science **282**, 1660 (1998); Y. Ohno et al., Nature (London) **402**, 790 (1999)
6. R.K. Kawakami et al., Science **294**, 131 (2001)
7. C. Ciuti, J.P. McGuire, L.J. Sham, Phys. Rev. Lett. **89**, 156601 (2002)
8. A. Brataas, Y. Tserkovnyak, G.E.W. Bauer, B. Halperin, Phys. Rev. B **66**, 060404 (2002)
9. Q.F. Sun, H. Guo, J. Wang, Phys. Rev. Lett. **90**, 25830 (2003)
10. W. Long, Q.F. Sun, H. Guo, J. Wang, Appl. Phys. Lett. **83**, 1397 (2003)
11. J.X. Zhu, A.V. Balatsky, Phys. Rev. Lett. **89**, 286802 (2002)
12. B. Wang, J. Wang, H. Guo, Phys. Rev. B **67**, 092408 (2003)
13. E.I. Rashba, Phys. Rev. B **70**, 161201(R) (2004)
14. S.I. Erlingsson, J. Schliemann, D. Loss, `cond-mat/0406531`; B.A. Bernevig, `cond-mat/0406153`
15. A.-P. Jauho, N.S. Wingreen, Y. Meir, Phys. Rev. B **50**, 5528 (1994)
16. H.K. Zhao, G.v. Gehlen, Phys. Rev. B **58**, 13660 (1998); H.K. Zhao, Phys. Rev. B **63**, 205327 (2001); H.K. Zhao, J. Wang, Phys. Rev. B **64**, 094505 (2001)
17. Q.F. Sun, J. Wang, T.H. Lin, Phys. Rev. B **59**, 3831 (1999)
18. R. Landauer, IBM J. Res. Dev. **1**, 223 (1957); M. Büttiker, Phys. Rev. Lett. **57**, 1761 (1986)
19. H.K. Zhao, Z. Phys. B **102**, 415 (1997); H.K. Zhao, Phys. Lett. A **226**, 105 (1997)
20. M.H. Pedersen, M. Büttiker, Phys. Rev. B **58**, 12993 (1998)